Experimental Measurements and Monte-Carlo Simulation of Water Diffusion into Epoxy Matrices

M. S. MAJERUS, D. S. SOONG, and J. M. PRAUSNITZ, *Department of Chemical Engineering, University of California, Berkeley, California 94720*

Synopsis

Sorption and desorption data are reported for water in epoxy at 25°C and 70°C. A Monte-Carlo model based on the dual-sorption theory is formulated to explain observed diffusion behavior. Random walk of particles is followed through a regular lattice with randomly distributed adsorption sites. Comparison of predicted results with experiment shows that the model predicts sorption data well. A modification to the model is proposed to improve prediction of desorption data.

INTRODUCTION

Epoxies are used extensively as adhesives and in matrices for composite materials. Increased use of epoxies in structural applications makes accurate prediction of their service life important. Prediction of service life is difficult since many environmental factors affect sample durability. The most critical problem is moisture absorption, which significantly deteriorates the mechanical properties of the epoxy.[1-4]

This work reports moisture sorption data for tetrafunctional tetraglycidyl-4-4′-diaminodiphenyl-methane epoxy (TGDDM) cured with diaminodiphenyl sulfone (DDS); Figure 1 shows the major starting materials. This epoxy is lightly cross-linked because of steric and diffusional restrictions during cure.[2,5] It exhibits a broad glass-transition around 250°C.

Moisture-induced degradation of epoxies is not well understood. Researchers agree that water causes reversible plasticization of epoxy[1-3,5-7] but have not resolved the nature of epoxy–water interactions. Some experimental studies indicate that water interacts at specific segments of the epoxy, whereas others indicate that water collects in microvoids within the sample.

Dynamic mechanical measurements by Keenan and Seferis[6] identified two secondary transitions which depend on moisture content. The first transition occurs at 100°C; it both broadens and shifts with increasing moisture content. The broadening was attributed to moisture adsorbed preferentially in regions of low crosslink density of the epoxy. The second transition occurs at −50°C; moisture has a plasticization effect on this transition. Because the second transition was attributed to the rotational motion of the glycidyl portion of the epoxide group, plasticization with increasing moisture content indicates that water interacts with a specific site within the polymer. NMR studies by Moy and Karasz[7] show that in samples containing less than 1% moisture, water is localized at specific

Journal of Applied Polymer Science, Vol. 29, 2453–2466 (1984)
 CCC 0021-8995/84/082453-14$04.00

TGDDM (tetrafunctional tetraglycidal 4,4′ diaminodiphenyl methane epoxy)

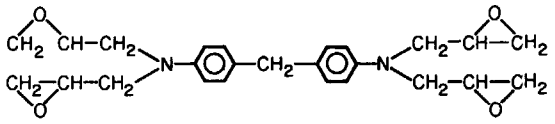

DDS (diaminodiphenyl sulfone)

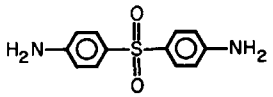

Fig. 1. Starting materials for TGDDM–DDS epoxy.

epoxy sites. Their IR studies suggest that this specific interaction is a result of hydrogen bonding.

Scanning electron microscopy by Browning[1] showed microcracking in epoxies which had been exposed to water and thermal spikes. Epoxies exposed to water but not thermal spikes showed areas of compression caused by swelling stresses. Electron microscopy studies by Morgan et al.[3] showed no microcracking. Electron diffraction data by Morgan et al.[5] showed that DDS crystalline regions are present in TGDDM–DDS samples when at least 25% DDS was used in the polymerization. Weight loss was observed as the annealing temperature increased, suggesting that the unreacted DDS was eliminated during annealing. Increased sorbed moisture with increasing anneal temperature was attributed to microvoids produced by elimination of DDS clusters. Repeated equilibrium sorption isotherms determined on the same sample by Apicella et al.[8] indicated that water irreversibly damages epoxy. During their first set of sorption runs, the sorption isotherm showed positive deviations from linearity. Upon subsequent sorptions of the same sample, the sorption isotherm was linear and above the original curve.

The diverse and seemingly conflicting experimental data suggest that under some conditions water interacts with segments of the epoxy, while under other conditions water collects in microvoids. A model which predicts water diffusion in epoxy must accommodate both types of epoxy–water interactions.

Below its glass-transition temperature, the diffusion characteristics of water in epoxy are believed to be non-Fickian.[2,7,8] Diffusion data show that Fick's law is an acceptable approximation under certain circumstances.[2,3,9–11] A plot of sorbed moisture vs. the square root of time is linear initially, as predicted by Fick's law. Deviations from Fick's law are apparent at longer times. Several workers have measured diffusion and equilibrium sorption of moisture.[1,3,7,8–11] These studies are useful for prediction of diffusion behavior under a particular set of conditions. Although all workers agree that severe environmental conditions increase moisture sorption, their equilibrium sorption and diffusion data do not agree well quantitatively, probably because of differences in sample composition and history.

Few attempts have been made to model moisture sorption. The observed Fickian diffusivity can vary by several orders of magnitude depending on

the researcher.[3,10,11] McKague et al.[10] correlated equilibrium-sorption data as a function of humidity using a power law. They reported a wide variation in the power among literature data. Shen and Springer[11] used a power-series solution of Fick's law to estimate diffusion curves of epoxy composites at long times. Weitsman[12] modeled the diffusion behavior of epoxies exposed to a thermal spike using a time-varying diffusivity. Apicella et al.,[13] who proposed a history-dependent diffusivity, modeled moisture-induced damage as Langmuir sites and calculated an effective diffusivity.

Dual-sorption theory uses the concept of microvoids to account for the shape of the sorption isotherm for glassy polymers.[14,15] This theory divides the solubility into two parts: ordinary sorption throughout the polymer and adsorption at specific sites. Henry's law represents ordinary sorption; a Langmuir isotherm represents adsorption at specific sites. Dual-sorption theory also can be used to explain the diffusion behavior of fluids in glassy polymers.[15,16] For example, Vieth and Sladek[16] modeled diffusion assuming irreversible adsorption; the resulting diffusion equation must be solved numerically. Extensions of the model to include only partial immobilization increase mathematical complexity.[17,18]

In this work, a generalized version of the dual-sorption model is applied to sorption and desorption of water into epoxy. The objective is to predict the diffusion behavior of water in the epoxy under a variety of conditions. The proposed model is consistent with experimental data on epoxy–water interactions. Water interacting at specific sites within the polymer is distributed throughout the sample and accounted for by ordinary sorption. Water collecting in microvoids is accounted for by adsorption at specific sites. Note, however, that the physical nature of these specific sites, or traps, is not conclusively known. The sites may represent microvoids indeed, but could also be less accessible H-bond sites with associated tortuous diffusion paths in which water molecules are tightly bound. The proposed model is implemented with a Monte-Carlo computer simulation which models diffusion into a homogeneous solid with randomly distributed, reversible adsorption sites.

Experimental sorption and desorption data are given for 25°C and 70°C. Through adjustment of model parameters, the experimental data are fitted. The physical significance of the model parameters provides a qualitative understanding of the diffusion mechanism. This model allows prediction of moisture sorption under a variety of conditions, using only a few experimental measurements.

EXPERIMENTAL

Materials and Procedure

Fiberite 934 epoxy resin was made by reacting TGDDM (63.2 wt %) and DDS (25.3 wt %) using a BF_3 catalyst complex (0.3 wt % $CH_3CH_2NH_2/BF_3$). A small amount (11.2 wt %) of the epoxy in the difunctional form was also added to reduce crosslinking. The sample was cured and annealed in a reproducible manner. Details of the polymerization are reported elsewhere.[19] Samples provided by NASA in sheets with thickness ranging from 0.06 to 0.065 cm were cut into rectangular sections.

The samples were dried to constant weight in a vacuum oven at 70°C; usually 2 weeks were required. The sample thickness was measured with a micrometer; each sample was then placed in a constant-temperature water bath at 25°C or 70°C to begin the sorption run.

Sorption data were obtained by weighing the samples with a Sartorius analytical balance. The sample was taken from the water bath, blotted dry, and weighed after 5 min to allow surface water to evaporate completely. Since the diffusion process is slow, the absorbed moisture content is not affected by sampling and weighing. Each sample was kept in the bath until the sorption curve approached a plateau. The sample typically remained in the bath for 60–90 days.

Desorption was measured after the sorption curve approached a plateau. Each sample was placed in a vacuum oven at the same temperature as that of the water bath. Weight loss was measured as a function of time.

Experimental Results and Discussion

Figures 2 and 3 show sorption and desorption behavior for several samples at 25°C and at 70°C. Both curves show wt % moisture divided by equilibrium moisture sorption, C/C_∞, vs. the square root of time divided by sample thickness, $\sqrt{t}/l$.

The sorption curves are linear initially; then, the slope decreases and the curve asymptotically approaches a plateau. Leveling of the curves is more gradual than that predicted by Fick's law. Desorption is initially more rapid than sorption; however, in midrange it slows, and the two curves cross. Crossing occurs at shorter times for the 25°C run than for the 70°C run. At both temperatures, the desorption curve levels before the sample completely dries.

Equilibrium sorption was also measured at both temperatures; it is 6.0 wt % at 25°C and 7.8 wt % at 70°C.

Since the edge effect is neglected, 1-dimensional diffusion can be used in the analysis of the sorption curves. This is a good approximation because the sample length and width are much larger than the thickness. The diffusion process is subject to the following boundary conditions: For $t < 0$,

$$C = 0 \qquad \text{at } -l/2 \leq x \leq +l/2$$

For $t > 0$,

$$C = \text{const} \qquad \text{at } x = l/2$$

$$\partial C/\partial x = 0 \qquad \text{at } x = 0$$

where l = sample thickness, $x = 0$ at center line, and C = moisture content. Fickian diffusion can be assumed in the range where the sorption curves are linear. This allows the following approximation at short times[20]:

$$\frac{C}{C_\infty} = \frac{4\sqrt{Dt}}{\sqrt{\pi}\, l} \tag{1}$$

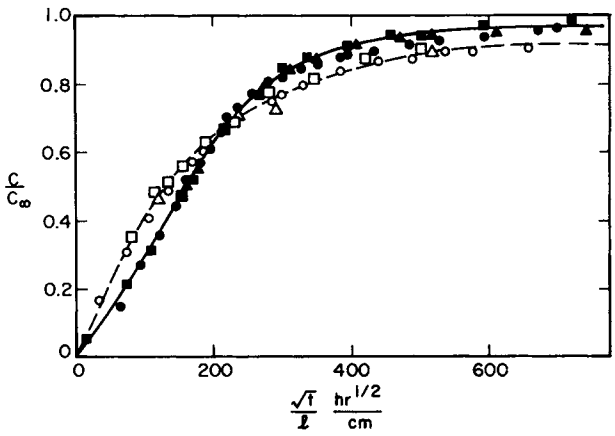

Fig. 2. Experimental sorption and desorption at 25°C: (——) sorption; (– – –) desorption; symbols indicate data for three different runs.

Diffusivities D at 25°C and 70°C can then be calculated from the initial slope of the sorption curves, using eq. (1). The activation energy E for diffusion can be calculated using an Arrhenius relation,

$$D = D_0 \exp(-E/RT) \tag{2}$$

These calculations yield $E = 8806$ cal/g · mol and $D_0 = 1.56 \times 10^{-3}$ cm²/s. These results compare favorably with data reported by McKague et al.[9]: $E = 8063$ cal/g · mol and $D_0 = 5.14 \times 10^{-4}$ cm²/s.

When C/C_∞ is greater than 0.6, the behavior of the sorption curves can be attributed to a concentration-dependent diffusivity or to microvoids within the epoxy. The rapid rise in the desorption curve and subsequent crossing of the sorption curve suggest that the diffusivity first increases with concentration, goes through a maximum and then decreases.[21] An alternative explanation is that as the concentration of water increases, it collects in

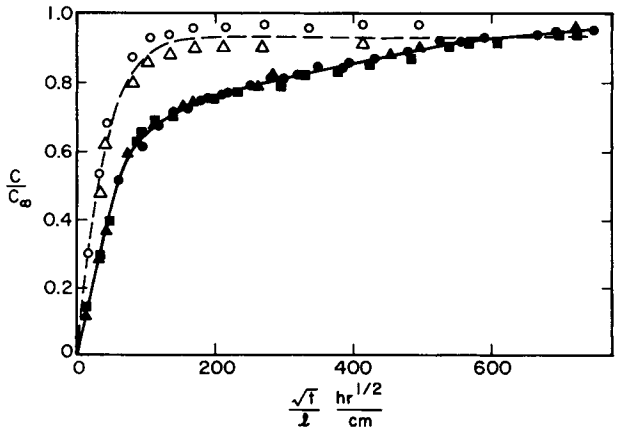

Fig. 3. Experimental sorption and desorption at 70°C. The symbols are the same as those in Figure 2.

traps in the epoxy matrix. This second explanation is preferred because it can describe the hysteresis of repeated sorption and desorption curves.

COMPUTER MODELING

Monte-Carlo Simulation

King[22] suggested in 1951 that Monte-Carlo simulation be applied to diffusion problems. He described an algorithm for diffusion into a homogeneous solid which yields Fick's law.[23,24] While most of the diffusion processes previously simulated by the Monte-Carlo method are equivalent to Fick's law, this method is also useful for more complex diffusion processes.[25] In many cases, it is easier to simulate a complicated diffusion problem than to solve the equivalent differential equation numerically.

The Monte-Carlo method assumes that molecules diffuse via a random walk with each step independent of the previous step. The simplest approach is to construct a regular lattice and to assume that, at each step, a particle moves from one lattice point to an adjacent lattice point. For example, in a simple 3-dimensional solid, the particle can move in six directions.

The main problem with Monte-Carlo simulations is that the required computing time is large. Even when a relatively small lattice size is used, e.g., $20 \times 20 \times 20$, many repeated calculations are required. If 6% of the lattice points contain particles at equilibrium, steps must be generated for up to 480 particles per iteration. An iteration is defined as one jump per particle. More than 4900 iterations are required for this lattice to reach equilibrium.

In this work, Monte-Carlo simulation is used to study diffusion according to the dual-sorption theory. The simulation uses a homogeneous set of lattice points with randomly distributed traps of a specified capacity. Adsorbed molecules in traps can have any desired degree of reversibility. The reversibility is defined as the chance that an adsorbed particle leaves a trap. For example, a reversibility of 0.25 means that a particle has a one-in-four chance of leaving the trap in a given iteration.

To allow comparison of the model with diffusion data, the simulation uses the boundary conditions shown in Figure 4. A 3-dimensional $20 \times 20 \times 20$ lattice is used. Periodic boundary conditions are used for two of the dimensions to represent the infinite length and width of the sample. The constant concentration of water at the lattice surface is simulated by setting the number of water particles on the first row of the lattice to a constant equilibrium value. The symmetry of the problem is accounted for by assuming the last row to be a perfect reflector. The last row of the lattice represents the midplane of the sample.

The number of water particles in the model at equilibrium is set by the equilibrium sorption data. The solubility is converted to volume percent by assuming that the density of water and epoxy are equal.

Consideration is given to two types of sorbed-water molecules: those in the bulk matrix and those in traps. For example, in a $20 \times 20 \times 20$ lattice, a water solubility of 6% means that, at equilibrium, there are 480 particles in the lattice. The number of water particles in traps and the number of water particles in the bulk must be specified. For example, the 6% water

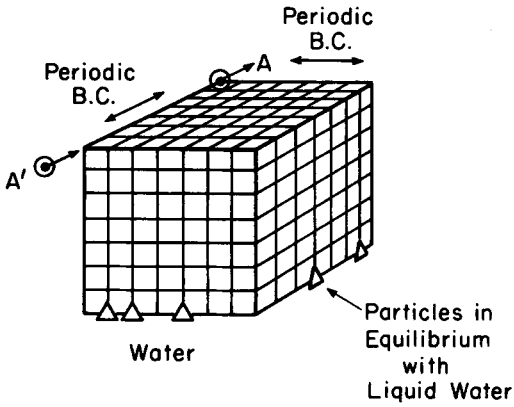

Fig. 4. Model lattice and boundary conditions. This is a 7 × 7 × 7 schematic representation. In the actual simulation, a 20 × 20 × 20 lattice is used. The periodic boundary condition specifies that as particle A leaves the back of the lattice, particle A' enters the front. The bottom plane is exposed to liquid water, while the top reflector represents the midplane of the sample.

could consist of 4% in the bulk and 2% in traps. In this case, at equilibrium, there are 320 particles in the bulk and 160 particles in traps.

After dividing the solubility into two parts, it is necessary to set the first-row concentration, the percentage of traps, trap capacity, and trap reversibility. Table I shows the relation between the variables by giving sample values. The first-row concentration equals the solubility of water in the bulk. It is assumed that there are no traps in the first row. The percentage of traps is the percentage of the total number of lattice points which are traps. The trapped water at equilibrium is the product of the traps and trap capacity, expressed as a percent or a number. If the trap capacity is multiplied by the percentage of traps, the percent trapped water at equilibrium is found. Multiplying the trap capacity by the number of traps yields the number of trapped particles at equilibrium. Before the calculations begin, the traps are randomly positioned in the lattice and, as determined by the bulk solubility, the particles are randomly placed in the first row.

The simulation begins by moving each particle in a direction corresponding to a random integer from 1 to 6. After each particle has moved, equilibrium is restored to the first row. The number of required iterations rises with the total number of trapped particles and with the reversibility of the traps.

TABLE I
Sample Input Variables for Monte-Carlo Simulation (20 × 20 × 20 Lattice)

	Percent	No. of particles
Total solubility	6	480
Bulk solubility	4	320
Trapped water at equilibrium	2	160
First-row concentration	4	16
Traps	1	80
Trap capacity	—	2

After a sorption simulation ends, calculations are made for desorption. The particles start in their final sorption positions and the equilibrium concentration of particles in the first row is set to zero. The reversibility of the traps remains unchanged.

Model Parameters

Several parameters must be determined to compare calculated with experimental results. These parameters include a conversion factor (discussed below), trapped water at equilibrium, and reversibility of the traps.

The conversion factor is needed to convert calculated Monte-Carlo results (units of steps$^{1/2}$/lattice size) into real time (units of h$^{1/2}$/cm). This temperature-dependent conversion factor is readily determined from the initial slope of the sorption curves. The other parameters define the state of the sample and are more difficult to specify quantitatively.

Trapped water at equilibrium is the product of the trap capacity and trap percentage. For the low percentage of traps used in this study, diffusion behavior is significantly affected by the trapped water at equilibrium, not by the trap percentage. Trapped water at equilibrium gives an estimate of the damage the sample has sustained. If moisture sorption increases damage, the water solubility in traps must be raised to model subsequent sorption curves. Reversibility is the probability that a trapped particle leaves a trap. A reversibility of zero indicates total immobilization; a reversibility of unity is equivalent to no traps.

The trapped water at equilibrium is a function of sample damage. Since the rate of sample damage due to water sorption is expected to be slow, it is assumed to be constant throughout a given sorption run. The sample damage or trapped water at equilibrium is also assumed to be independent of temperature for the temperature range explored in this work. However, the reversibility of the traps is a function of the mobility of the particles and would be expected to increase with temperature.

Since the lower-temperature data are less dependent on reversibility, these data are used to determine the trapped water at equilibrium. A reasonable value for the trapped water at equilibrium is chosen and a corresponding sorption curve is calculated, assuming irreversible traps. The calculated curve is then superimposed on the experimental plot, using the previously determined conversion constant. The time at which the two curves approach equilibrium is noted. The trapped water at equilibrium is adjusted until the best fit of the experimental data is obtained.

After finding the best fit for the trapped water at equilibrium, the reversibility is found by trial and error. The optimal reversibility is chosen in such a way that calculated and experimental curves coincide. In this process, if the experimental sorption curve approaches equilibrium more slowly than the calculated curve, the reversibility is increased and vice versa.

Simulation Results and Discussion

Simulations were run to verify the basic assumptions in the Monte-Carlo model and to quantify the effect of the different parameters on the sorption curves. First, the optimum lattice size must be determined. The model lattice size was picked by trial and error. A small lattice size is advantageous

because it requires less computer time; however, the lattice size must be large enough such that the results are not size-dependent. A simulation using a 30 × 30 × 30 lattice gave the same sorption behavior as that using a 20 × 20 × 20 lattice, suggesting that the 20 × 20 × 20 lattice is sufficiently large.

The scatter of the simulation results was estimated by running several simulations with the same parameters. The variation is about 20%. Since the scatter is due mainly to statistical fluctuations, a smooth average curve can be drawn using results from only a few simulations. The additional error introduced by assuming that the density of water is equal to that of epoxy was also estimated. Since the densities of water and epoxy are used to convert the experimental solubility from weight percent to volume percent, error in the density affects the total solubility assumed in the simulation. The error depends on the effect of solubility on the sorption results. As the solubility rises, there is a slight increase in the initial slope of the curve. This affects the calculated conversion constant. The resulting variation in the constant is less than 5%.

To test the assumption that the curves remain unchanged with constant product of percentage of traps and capacity, several simulations were run using 2% trapped water at equilibrium. Simulations ranged from 2% traps with a capacity of unity to 0.1% traps with a capacity of 20. All simulated sorption curves were the same within the error of the simulation.

Figure 5 shows the effect of trapped water at equilibrium on the simulated results. Simulation with no traps yields a curve which follows Fick's law. As the percent trapped water at equilibrium rises, the initial slope decreases, and the curve approaches equilibrium more slowly. Since the total solubility is kept constant, raising the trapped water at equilibrium decreases the bulk solubility. The lower bulk solubility, and therefore reduced first-row equilibrium, produces a decrease in initial slope. Slower approach to equilibrium follows from the long time required to fill the traps.

Figure 6 shows that the reversibility has only a modest effect on the initial slope but a large influence on the shape of the sorption curve. The initial slope is expected to remain relatively constant because the first-row

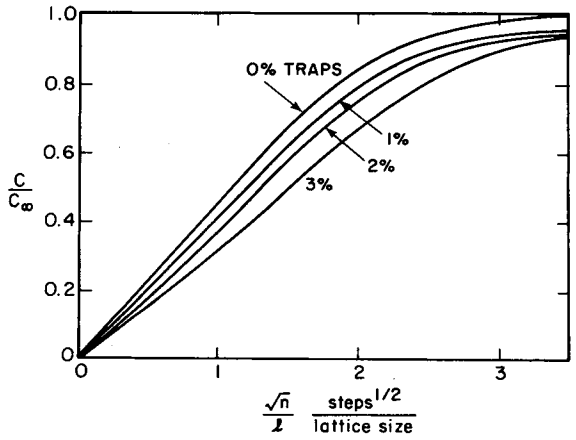

Fig. 5. Calculated sorption curves for different values of trapped water at equilibrium. Total equilibrium sorption is 6%. Each trap is irreversible with a capacity of 1.

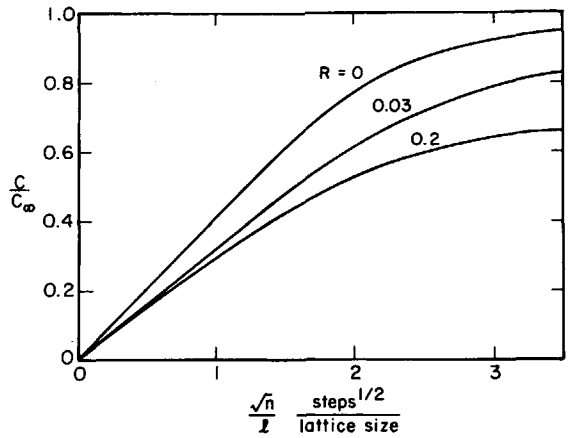

Fig. 6. Effect of reversibility R on calculated sorption curves. Total equilibrium sorption is 6%. Each simulation has 1% traps with a capacity of 2.

equilibrium does not vary with reversibility. When the reversibility is high, there are fewer particles in traps at any given time. A high reversibility, therefore, produces a slower approach to equilibrium.

Figure 7 shows that, in desorption, the reversibility has a much larger influence on the initial slope. Since the traps are initially at maximum water content, the trapped particles have an immediate effect on the desorption behavior. Since the rate at which the traps empty depends on the reversibility, a high reversibility is expected to speed desorption. This effect is opposite to that of reversibility on sorption. A sample with irreversible traps never dries completely because no trapped particle can escape.

RESULTS AND DISCUSSION

Table II shows parameter values used to fit experimental data. Uncertainty in the parameter values is large. The error in the conversion constant

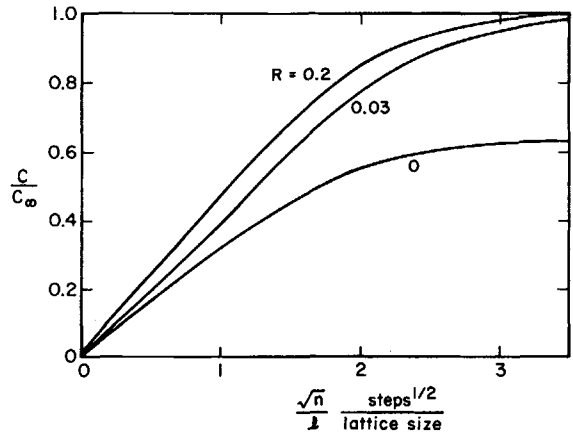

Fig. 7. Effect of reversibility R on calculated desorption curves. Total equilibrium sorption is 6%. Each simulation has 1% traps with a capacity of 2.

TABLE II
Parameters Used to Fit Experimental Data

Temp (°C)	Trapped water at equilibrium (%)	Conversion constant (lat size $h^{1/2}$/cm steps$^{1/2}$)	Reversibility
25	2	120	0.003
70	2	42	0.31

depends on the error in the initial slopes of the calculated and experimental curves. The estimated error in the constant is 15%.

By varying the reversibility, there are several possible values of trapped water at equilibrium which give comparable fits to the experimental data. The trapped water at equilibrium is greater than zero because the experimental curve cannot be fitted using a simulated curve with no traps. On the other hand, the upper bound of trapped water at equilibrium is the point where the calculated curve falls below the experimental curve. Since rising reversibility slows the approach to equilibrium, predictions lower than the experimental data cannot be corrected. Using these criteria, the trapped water at equilibrium is between 0% and 4%. 2% water at equilibrium gives the best fit of the 25°C data, assuming nearly irreversible traps.

The uncertainty in the reversibility depends on the uncertainty of the trapped water at equilibrium because it is fixed last. Since the shape of the sorption curve is more sensitive to the reversibility than to the trapped water at equilibrium, reversibility varies little with trapped water at equilibrium. For example, the reversibility decreases only slightly from 0.003 if 3% trapped water at equilibrium is used rather than 2%. A high reversibility is needed to fit 70°C data regardless of the trapped water at equilibrium.

Figures 8 and 9 show a comparison of calculated and experimental sorption and desorption for 25°C and 70°C. The points represent experiment. The 70°C simulated curves stop at a C/C_∞ of 0.7 because the computer costs become prohibitive for a higher C/C_∞.

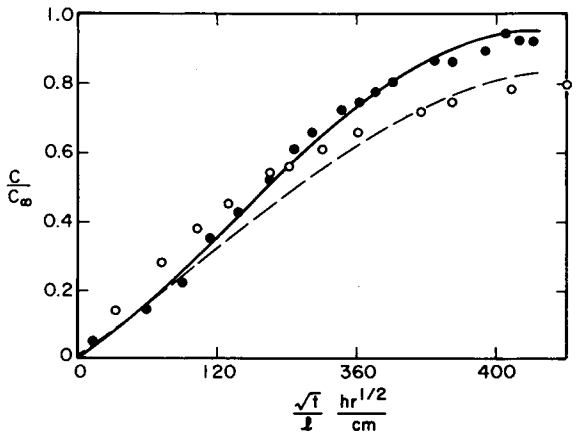

Fig. 8. Comparison of experimental and calculated results at 25°C: (———) calculated sorption; (– – –) calculated desorption; (●) experimental sorption data; (○) experimental desorption data.

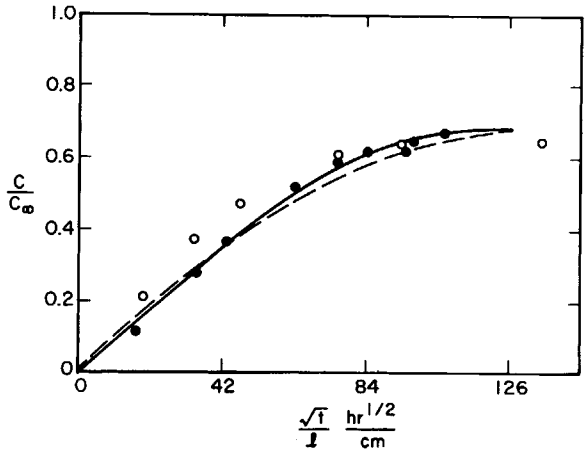

Fig. 9. Comparison of experimental and calculated results at 70°C. Symbols are the same as those in Figure 8.

Model results agree well with experimental sorption data. The different shapes of the sorption curves at two temperatures are easily explained by a temperature-dependent reversibility. The 25°C curve appears to level whereas, even after long times, the 70°C curve maintains an upward slope. Since, at 25°C, the traps are nearly irreversible, they fill quickly and the approach to equilibrium is rapid. At 70°C, the same traps are filled and emptied repeatedly; therefore, the net approach to equilibrium is expected to be slower.

Calculated curves for desorption agree qualitatively with experiment. The desorption curve rises more quickly than the corresponding sorption curve initially, but subsequently the rise slows and the curves cross. Calculated curves at 25°C cross at an earlier time than those at 70°C, as in the experimental plots. Quantitative agreement is poor, however. At both temperatures, the model prediction is too low at short times and too high at long times. Crossing of the experimental sorption and desorption curves occurs at longer times than those predicted by the model.

The only way to approximate the initial slope of the experimental desorption curve is to increase the reversibility. A simulation using a reversibility of unity approximates the initial slope of the experimental desorption curves but at longer times the prediction is too high. This suggests that the reversibility may not be a constant; the reversibility fit to the sorption curve represents an average value.

An average reversibility can be used to fit sorption but not desorption because reversibility has a much larger effect on the initial slope of the desorption curve. The initial slope of the simulation sorption curve fits the initial slope of the experimental curve, using a conversion constant. Since, in sorption, the initial slope does not vary much with reversibility, the reversibility can be fitted to the data with little change in the conversion constant. If the same conversion constant is used in desorption, the model underpredicts experiment. If the desorption initial slope is fitted to a different conversion constant, the desorption simulation overpredicts at long times. When the reversibility is decreased to fit the curve at long times, the slopes of the experimental and calculated curves do not coincide. Be-

cause of the large change in the initial slope with reversibility, both short and long times cannot be fitted with the same reversibility. If a varying reversibility is used, both sorption and desorption data can be predicted.

A variable reversibility at a constant temperature can be explained physically if there is a strong interaction between the trapped water and localized sites. In this case, the traps interact strongly with the initially adsorbed particles, corresponding to a reversibility close to zero. As the trap fills, the water particles interact more with other water particles and reversibility increases. Similarly, in desorption, reversibility is initially close to unity and then decreases as the traps are emptied. This would explain the leveling of the experimental desorption data at a water content greater than zero (see Figs. 2 and 3).

A variable reversibility can be added to the model by assuming the traps to be Langmuir sites, as suggested by the dual-sorption theory. To be consistent with the Langmuir model, trap capacity is defined as the number of possible adsorption sites in the trap. The fraction of filled sites, θ, equals the number of particles in the trap divided by trap capacity. The reversibility, or chance that a trapped particle leaves a trap, is the same as the number of particles leaving a trap divided by the number of adsorbed particles. Therefore, a Langmuir-type reversibility is defined as the rate of desorption divided by the total number of adsorbed molecules. In the Langmuir model,

$$\text{rate of adsorption} = k_1 P(1-\theta)$$

$$\text{rate of desorption} = k_{-1}\theta$$

$$\text{reversibility} = \theta/[b(T)\,P(1-\theta) + \theta]$$

where k_{-1} = desorption rate constant, k_1 = adsorption rate constant, P = gas pressure, and $b(T)$ = hole-affinity constant.

The temperature dependence of a Langmuir-type reversibility depends on the relative temperature dependence of the rate constants for adsorption and desorption. The advantage of the Langmuir model is that it has been successfully used in a dual-sorption theory to explain the diffusion behavior of other glassy polymer–fluid systems[15–18] and that it gives an analytical expression to relate reversibility to the fraction of the trap that is filled.

To apply the Langmuir model to the simulation, first the temperature-dependent equilibrium constant must be determined. This can be found from estimates of the adsorption and desorption rate constants or else the equilibrium constant can be considered an empirical parameter. Multiplying b by the vapor pressure at the diffusion temperature allows the pressure to be replaced with an activity, defined as pressure divided by the vapor pressure. For liquid water diffusion, the activity equals unity.

To explain the discrepancy between simulated and experimental desorption, additional experimental information is needed on the structure of the epoxy and on epoxy–water interactions. It will be useful to understand better the nature of epoxy chemistry and structure before and after water sorption. Some possible tests would be provided by infrared spectroscopy, NMR, and electron microscopy. These tools have already been used sepa-

rately,[3-5,7] but, to make significant progress, it will be necessary to integrate results from a variety of experimental studies.

CONCLUSIONS

Sorption and desorption data are reported for water in epoxy at 25°C and 70°C. A Monte-Carlo simulation is used to explain diffusion behavior, assuming the existence of traps, i.e., localized regions of water. The three parameters used are a conversion constant, trapped water at equilibrium, and reversibility. Trapped water at equilibrium is a measure of the damage of the sample; reversibility is a measure of the ease with which water can leave a trap.

In its present form, the model can only be used to predict sorption data. Comparison of simulated desorption results with experiment suggests that when the traps are full, it is easier for water to escape than when they are empty. A variable reversibility at a constant temperature can be incorporated into the model by considering the traps to be Langmuir adsorption sites.

The authors would like to thank Dr. Eric Kong at NASA Ames Research Center for supplying the epoxy samples and Professor David Aldous of the Statistics Department at the University of California at Berkeley for helpful discussions. This work was supported by the Office of Naval Research.

References

1. C. E. Browning, *Polym. Eng. Sci.*, **18**, 16 (1978).
2. R. J. Morgan and J. E. O'Neal, *Polym. Plast. Technol. Eng.*, **10**, 49 (1978).
3. R. J. Morgan, J. E. O'Neal, and D. L. Fanter, *J. Mater. Sci.*, **15**, 751 (1980).
4. H. T. Sumsion, *J. Spacecraft Rockets*, **13**, 150 (1976).
5. R. J. Morgan, J. E. O'Neal, and D. B. Miller, *J. Mater. Sci.*, **14**, 109 (1979).
6. J. D. Keenan and J. C. Seferis, *J. Appl. Polym. Sci.*, **24**, 2375 (1979).
7. P. Moy and F. E. Karasz, *Polym. Eng. Sci.*, **20**, 315 (1980).
8. A. Apicella, L. Nicolais, G. Astarita, and E. Drioli, *Polymer*, **22**, 1064 (1981).
9. E. L. McKague, J. E. Halkias, and J. D. Reynolds, *J. Comp. Mater.*, **9**, 2 (1975).
10. E. L. McKague, J. D. Reynolds, and J. E. Halkias, *J. Appl. Polym. Sci.*, **22**, 1643 (1978).
11. C. H. Shen and G. S. Springer, *J. Comp. Mater.*, **10**, 2 (1976).
12. Y. Weitsman, *J. Comp. Mater.*, **10**, 193 (1976).
13. A. Apicella, L. Nicolais, G. Astarita, and E. Drioli, *Polym. Eng. Sci.*, **21**, 18 (1981).
14. H. L. Frisch, *Polym. Eng. Sci.*, **20**, 2 (1980).
15. W. R. Vieth, J. M. Howell, and J. H. Hsieh, *J. Membr. Sci.*, **1**, 177 (1976).
16. W. R. Vieth and K. J. Sladek, *J. Colloid Sci.*, **20**, 1014, (1965).
17. D. R. Paul and W. J. Koros, *J. Polym. Sci.*, **14**, 675 (1976).
18. J. H. Petropoulos, *J. Polym. Sci., Part A-2*, **8**, 1797 (1970).
19. E. S. Kong, *Comp. Tech. Rev.*, **4**(3), 97 (1982).
20. J. Crank and G. S. Park, *Diffusion in Polymers*, Academic, London, 1968.
21. J. Crank and M. E. Henry, *Trans. Faraday. Soc.*, **45**, 636 (1949).
22. G. W. King, *Ind. Eng. Chem.*, **43**, 2475 (1951).
23. G. E. Murch, *Am. J. Phys.*, **47**, 78 (1979).
24. G. E. Murch and R. J. Thorn, *Phil. Mag. A*, **39**, 673 (1979).
25. W. W. Brandt, *J. Chem. Phys.*, **59**, 5562 (1973).

Received August 24, 1983
Accepted January 14, 1984